The 3D DNS of a Taylor bubble in counter-current flow with a turbulent wake using the Front-Tracking method in TRUST/TrioCFD

Raksmy Nop, Grégoire Hamrit, Alan Burlot, Guillaume Bois, Blaz Mikuz, Iztok Tiselj

NENE
International Conference
Nuclear Energy for New Europe

The 3D DNS of a Taylor bubble in counter-current flow with a turbulent wake using the Front-Tracking method in TRUST/TrioCFD

Raksmy Nop[1], Grégoire Hamrit[1], Alan Burlot[1], Guillaume Bois[1], Blaž Mikuž[2], Iztok Tiselj[2]

[1]Université Paris-Saclay, CEA, Service de Thermohydraulique et de Mécanique des Fluides
F-91191 Gif-sur-Yvette, France
raksmy.nop@cea.fr

[2]Reactor Engineering Division, Jožef Stefan Institute
Jamova cesta 39
1000 Ljubljana, Slovenia

ABSTRACT

The understanding of two-phase flows is of key importance for the nuclear industry as they may occur in normal operation, like in the steam generators, or in accidental scenarios, like in the core during a loss of coolant accident (LOCA). Among the variety of regimes that may occur in a two-phase flow, there is the slug flow composed of different kind of patterns. One of them is the Taylor bubble which is a large bubble filling almost the entire section of the vertical channel in which it tends to rise up. The correct simulation of a Taylor bubble is challenging as it can be decomposed in three zones involving different scales and mechanisms.

In this communication, we present simulations of Taylor bubble experiments realized by the THELMA laboratory at the Reactor Engineering Division of Jožef Stefan Institute, Slovenia. These experiments were done using air-water mixture in a vertical pipe with a diameter of 12.4 mm. The simulations were realized with TrioCFD, the open-source CFD code developed at CEA, in Direct Numerical Simulation (DNS) using the Front-Tracking (FT) method for interface tracking. Note that this choice of DNS+FT to simulate a Taylor bubble is particularly scarce in the literature and is a premiere for such conditions.

INTRODUCTION

Two-phase flow can occur in many applications: hydrocarbon industry, computer cluster cooling and in the nuclear industry in the steam generators in normal conditions or in the nuclear core in accidental scenarios. Nonetheless, the understanding and the simulation of such flows are still challenging as there are different regimes depending on the vapor fraction (see. Figure 1) One of them is the so-called slug flow which is characterized by large vapor patches flowing in the pipe. The Taylor bubble is one of its characteristic pattern: this is a long bullet-shaped bubble taking almost the whole radius of the pipe. Understanding the behavior of the Taylor bubble is important for the nuclear safety as it may be involved in the core during a Loss of Coolant Accident (LOCA) in the core before the latter reach the boiling crisis.

The challenge in simulating a Taylor bubble is due to the involvement of different scales. Indeed, the flow around a Taylor bubble can be classified in three zones:

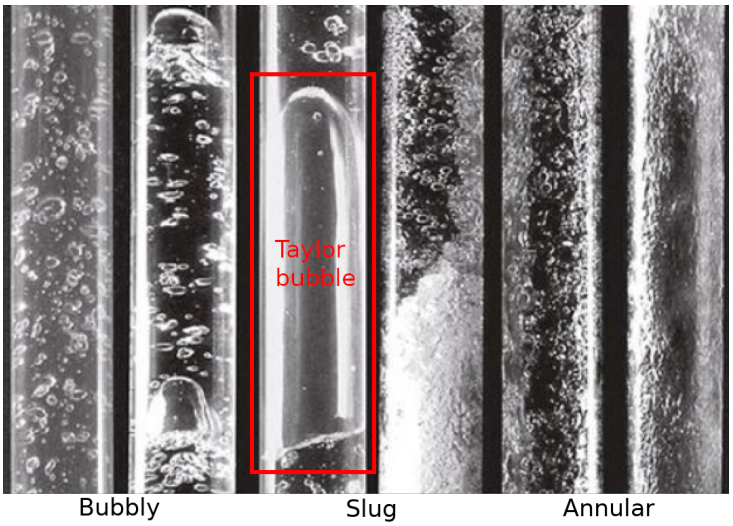

Figure 1: Photographs of different two-phase flow regimes

- The head. The flow coming from the top shapes the head of the bubble, whose the form has to be caught.
- The body. As the bubble almost takes the whole radius of the pipe, there is an annular-shape liquid film around the bubble. Predicting its thickness is of key importance as it determines the liquid film velocity and the pressure drop generated by the whole bubble.
- The tail. According to several non-dimensional quantities as N_f (see sections 1 and 3.3), the shape may differ and fragmentation can occur implying a decay in the bubble volume. Moreover, the wake can be laminar or turbulent.

In order to improve the slug flow models in averaged two-phase flow CFD codes, one needs to be able to predict the behavior of each of these zones as a function of the working parameters. One of the way to head to this objective is to realize "numerical experiments" with Direct Numerical Simulation (DNS). The simulation of Taylor bubbles has been widely investigated, but mostly using the Volume of Fluid (VOF) approach. One can for instance cite the simulations of Kren et al. [1]-[2] using Large Eddy Simulation (LES), or Frederix et al. [3] in DNS, but no DNS simulation using the Front-Tracking method has been reported.

In the present work, we present the DNS simulation of a Taylor bubble using the open-source code TRUST/TrioCFD. First of all, we present the case study which is an experimental measurement of a Taylor bubble realize at the TELMA laboratory at the Jožef Stefan Institute (JSI), Slovenia. The numerical setup will be then described and followed by analyses of the simulation results.

1 THE EXPERIMENTAL CASE OF STUDY

The THELMA laboratory at JSI has designed an experimental apparatus allowing for the investigation of stationary counter-current Taylor bubble [4]. The latter is made of a hydraulic loop with an air injection enabling to stabilize a bubble in the test section. The inner section of the test section is circular but the overall has a rectangular shape which allows a backlit shadowgraphy visualization with low optical distortion. Two test section diameters are available: 26 mm and 12.4 mm. In term of diagnostics, the apparatus can realize measurements of pressure drop, interface shape, liquid film thickness and PIV. Among the various experiments that have been conducted with this apparatus, we will in focus on the Taylor bubble in the 12.4 mm pipe. In such section diameter, the flow is laminar upstream the bubble, but the wake is turbulent. On table 1 is listed the key characteristics of the investigated conditions.

Table 1: Properties of the investigated Taylor Bubble

Mixture	Temperature $[^oC]$	Inlet Velocity $[m.s^{-1}]$	Re [-]	Eo [-]	Mo [-]	N_f [-]
Water/Air	29.5	9.3 10^{-2}	1423	21	1.2 10^{-11}	5342

with the Reynolds number $Re = \frac{U_{in}D}{\nu}$, the Eötvös number $Eo = \frac{\Delta\rho\ g\ D^2}{\sigma}$, the Morton number $Mo = \frac{g\mu_{water}\Delta\rho}{\rho_{water}\sigma^3}$, the inverse viscosity number $N_f = Eo^{3/4}Mo^{-1/4}$.

2 NUMERICAL SETUP

2.1 The opensource code TRUST/TrioCFD and its Front-Tracking method

TRUST/TrioCFD is an massively parallel open-source CFD code developed by the CEA since the 90s [5]. Historically designed for nuclear engineering and research applications, TRUST/TrioCFD is dedicated to simulate hydraulic and thermalhydraulic flow which can be slightly compressible, in single or two phase. It also has modules for chemistry applications and fluid-structure interactions. Among the various options that are offered by TRUST/TrioCFD, two-phase flow investigation can be conducted by using the Front-Tracking approach. The latter uses an Euler-Lagrange approach coupled with a Volume-of-Fluid method. It uses one-fluid formulation for the fluid mixture and an explicit interface tracking. By considering:

- the indicator function χ_k being 1 if the considered point is in the phase k and 0 otherwise,
- the variable ϕ_k (pressure, velocity, viscosity...) having its given value in the phase k.

One can define a one-fluid variable as $\phi = \sum_k \chi_k \phi_k$. Then, by summing the continuity equation for incompressible fluids and the Navier-Stokes equation for each phase and using the Laplace pressure law for the interface, one can derive the equation system:

$$\begin{cases} div(\vec{u}) = 0 \\ \rho\dfrac{\partial\vec{u}}{\partial t} + \rho\left(\vec{u}.\vec{\nabla}\right)\vec{u} = -\vec{\nabla}p + div\left[\mu\left(\vec{\nabla}\vec{u} + {}^t\vec{\nabla}\vec{u}\right)\right] + \rho\vec{g} + \sigma\kappa\delta_I\vec{n} \end{cases} \tag{1}$$

with $\vec{u}$ the velocity field, ρ the density, p the pressure, μ the dynamic viscosity, $\vec{g}$ the gravity field, σ the surface tension, κ the local curvature of the interface, δ_I the indicator function of the interface and $\vec{n}$ the vector normal to the interface.

Concerning the interface, its lagrangian mesh is advected between two time steps by an interpolation of velocity. A transport of the phase indicator function (similar to the Volume-of-Fluid resolution) coupled with the computation on the volume of gas are realized in order to ensure the mass conservation and the interface treatment is concluded by a smoothing and a remeshing.

2.2 Computational characteristics and methods

On figure 2a, we present the computational domain. This is a vertical circular pipe of a length $L = 10\ cm$ and of a diameter $D = 12.4\ mm$. Due to the Reynolds number involved in the experiments, the inlet flow is laminar and a Poiseuille velocity field is implemented as inlet conditions and a free pressure condition at the outlet. At the pipe wall, a no-slip condition is imposed. The properties of the fluids are taken at 29.5^oC and presented in table 2. Regarding the initial condition, the velocity field is set as a Poiseuille flow in the whole domain. As illustrated in figure 2a, the bubble is initiated as an hemisphere at the head, contiguous to a cylinder of a same radius letting a liquid film of a thickness δ chosen as 10% of the diameter. This is significantly larger than the real liquid film thickness, but it eases the initialisation

of the computation. Indeed, taking it too thin tends to break the bubble before reaching its steady-state shape.
The computational domain has been meshed using the internal mesh generator of TRUST/TrioCFD coupled with GMSH. The process starts with meshing a quarter of disc in two different section :

- a corona approximately twice the thickness of the measured liquid film filled with prisms whose size follows a geometrical expansion law. The latter are then cut to triangles.
- the bulk domain homogeneously filled with triangles.

The resulted mesh is extended to generate the circular pipe cross-section (see figure 2b) and extruded to generate the entire pipe. The final mesh is then constituted of tetrahedral elements.

Table 2: Fluid Properties implemented in the simulation

$\rho_{water}[kg.m^{-3}]$	$\rho_{air}[kg.m^{-3}]$	$\mu_{water}[kg.m^{-1}.s^{-1}]$	$\mu_{air}[kg.m^{-1}.s^{-1}]$	$\sigma[N.m^{-1}]$
995.8	1.202	8.0578 10^{-4}	1.8179 10^{-5}	7.0 10^{-2}

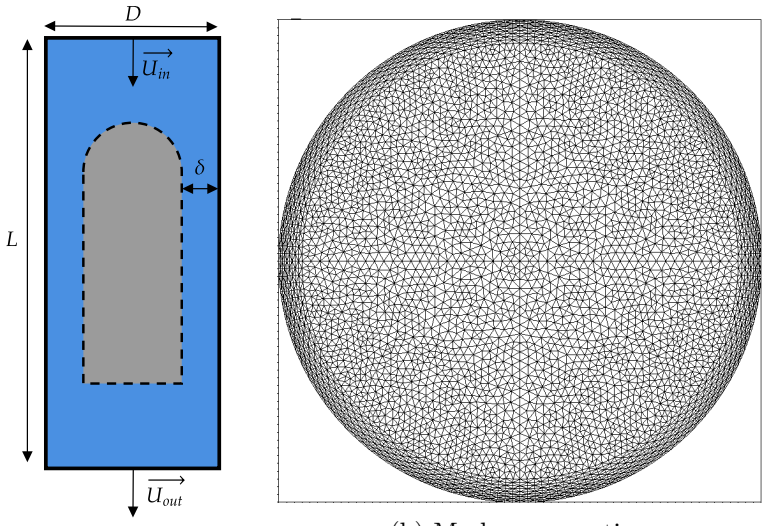

(a) Domain

(b) Mesh cross-section

Figure 2: Computational domain schematics at the initial time and mesh cross-section

Two meshes have been generated whose the characteristics are presented in table 3. In order to quantify the quality of theses meshes, we estimated the length of an tetrahedral element using $h = \frac{Volume}{max(Surface)}$. In table 2b are reported the minimum length h_{min} and the average length h_{avg}. These lengths are compared with the Kolmogorov length which is approximated here as $\eta = \frac{1}{2}DRe^{-3/4} = 2.7\ 10^{-5}\ m$. A more accurate way to compute η, especially in the turbulent wake would be to analyze the velocity fluctuation statistics. This would realized in a future work. For now, as these two quantities are of the same order of magnitude, we can reasonably assume that the mesh is sufficiently refined for a DNS simulation.

Table 3: Meshes properties

	elements	$h_{min}\ [m]$	$h_{avg}\ [m]$	$h_{min}/\eta\ [-]$	$h_{avg}/\eta\ [-]$
Mesh 1	2,128,500	1.5 10^{-5}	4.2 10^{-5}	0.56	1.6
Mesh 2	4,743,900	1.4 10^{-5}	2.7 10^{-5}	0.52	1.0

In term of numerical methods, an explicit Euler scheme has been used for the time integration. The space discretization has been realized using the Finite Element Volume approach

which is a mix between the Finite Element and the Finite Volume methods [5]. For Mesh 1, a time step was about 6.8 10^{-6} s and was computed with 64 CPU. For Mesh 2, a time step was about 2.5 10^{-6} s and was computed with 160 CPU.

3 SIMULATION RESULTS AND VALIDATION

JSI has measured in this pipe configuration bubbles with various lengths. In the present work we present the simulation of two bubbles: 1.5 D (using mesh 1) and 3.5 D (using Mesh 2). We have computed about 1 s of physical time for the first bubble and about 0.6 s for the second one. The validation is made throughout the bubble shape and film thickness. Velocity field are presented and analysed, but validation with PIV data will be presented in a future work.

3.1 General overview

The simulation starts with a transient phase where the bubble has its initial non-physical shape and tends to its steady-state shape as seen in figure 3. The bouncing phase where the tail center penetrates the bubble, as illustrated at 42 ms in figure 3, is the phenomenon governing the length of the transient. Due to the deformability of the bubble, the bouncing and thus the initial time depends on the bubble length. For longer bubble (e.g. more than 4 D), it might even fragment the bubble. A solution would be to impose a larger surface tension during this phase to ease and shorten the transition process.

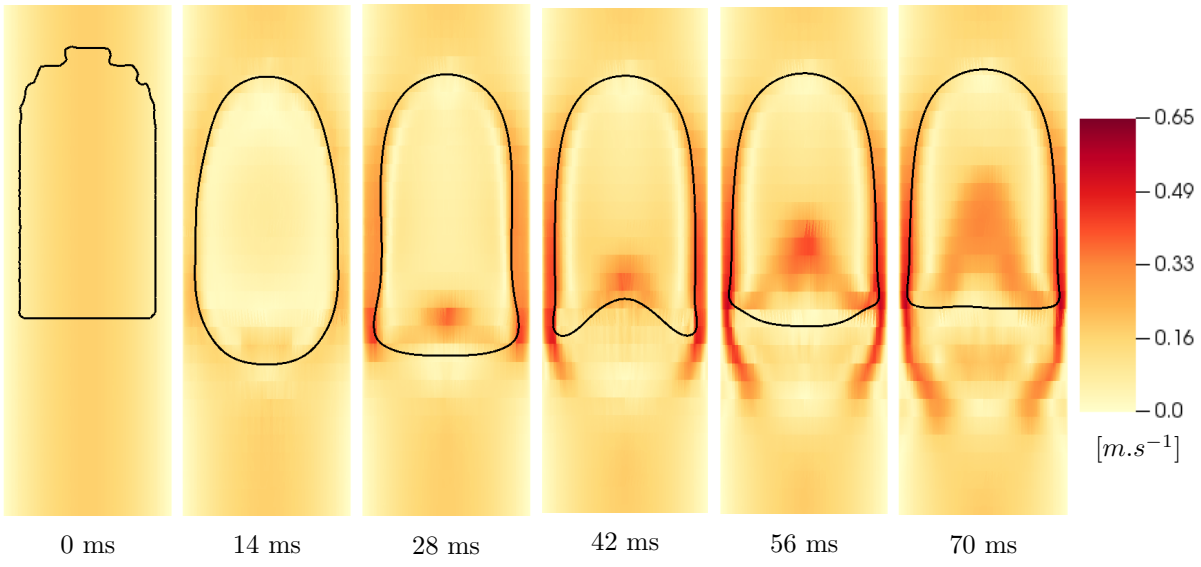

Figure 3: Initial transient phase of the simulation, case with a bubble with a length of 1.5 D

Once the Taylor bubble reaches its steady-state shape, we can observe that the bubble slightly rises during the rest of the simulation enlightening a discrepancy between the experiment where the bubble remains approximately steady. The rising velocity is 1.1 10^{-2} $m.s^{-1}$, or 12 % of the flowing velocity. This is acceptable knowing the 10 % measurement uncertainty and this provides a first element of validation.

3.2 Bubble shape and film thickness

The bubble shape is one of the most important characteristics to catch. Indeed, it affects the pressure drop induced by the bubble as well as the flow properties in the wake. Comparisons

between experimental measurement and simulation are presented in figure 4. Experimental measurements of the liquid film thickness have been produced using the process presented in Kren et al. [4]. For each stabilized bubble, 10 film thicknesses were measured, presented as the colored dots, that for both side (left and right) explaining the two thicknesses for each bubble. Regarding the film thickness resulted from simulations, the node coordinates of the interface mesh is simply extracted and displayed as the black dots in figure 4.

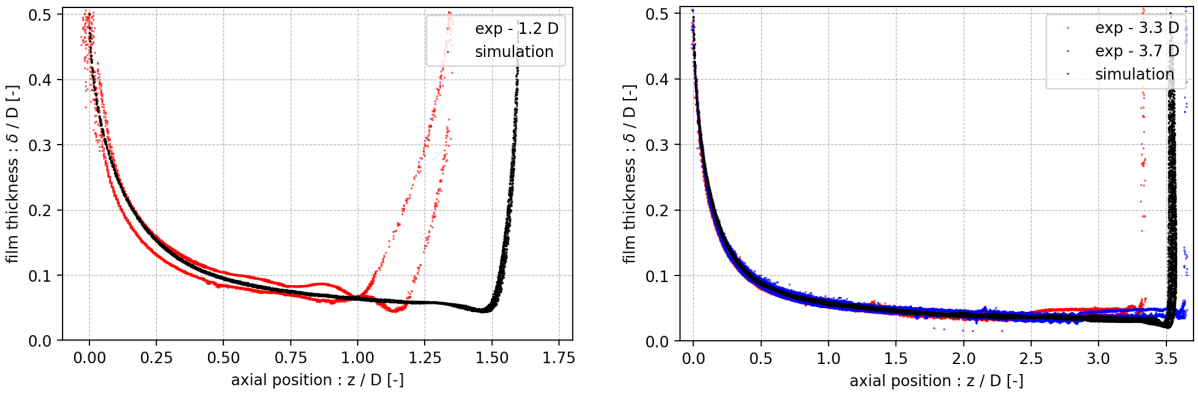

(a) 1.5 D long bubble

(b) 3.5 D long bubble

Figure 4: Liquid film thickness. The origin of the z-axis corresponds to the bubble head

The simulated bubbles are compared with the most relevant experimental bubble: the simulated bubble with a length of 1.5 D is compared with the experimental 1.2 D long bubble, and the simulated bubble with a length of 3.5 D is compared with the experimental 3.3 D and 3.7 D long bubbles. One can note that the bubble shape simulated by the Front-Tracking method is excellent as the latter were able to accurately reproduce all characteristics of the bubble. The liquid film thicknesses at the bubble body were perfectly reproduced for each case. At the bubble tail, we can also observe that the bump in the bubble shape is well predicted, as well as the bubble tail shape itself: convex for short bubbles (figure 4a) and (slightly) concave for longer ones (figure 4b). This is better illustrated in figure 5. Nonetheless, one can note that for long bubbles, e.g. 3.7 D long, experimental measurements show the presence of the stationary waves (between 2.2 and 2.7) then a thickening of the liquid film. Each of these phenomena at the bubble tail are not captured by our Front-Tracking simulation. This can be explained by the fact that the underlying mechanisms (most likely capillary waves) have length scales smaller that the one of the interface mesh and would anyway be mitigated by the smoothing process (see section 2.1). Finally, we can note that the nose shape is in overall really well capture, especially for the 3.5 D long bubble. Nonetheless, it seems that TRUST/TrioCFD tends to predict a head slightly more round that it should be: this is especially visible in figure 4a. This experimentaly validates the capability of TRUST/TrioCFD to predict the bubble shape.

3.3 Velocity field and bubble wake

On figure 5, we present an instantaneous velocity magnitude fields in the computational domain for each simulation (red and yellow maps). We can observe that, even though in overall the velocity field has same behavior for each length, the case with a 3.5 D long bubble shows larger magnitudes. This is due to a thinner liquid film at the tail (figure 4). We also represented the axial component of the velocity (red and blue maps), which enlightens a recirculation loop at vicinity of the bubble tails, but also inside the bubble. Subsequently, figure 5 shows that even though the inlet flow is laminar, a turbulent wake takes place behind the bubble tail. This is expected as inverse viscosity number N_f equals 5342 which is beyond the criterion of 1500 found by Campos and Carvalho [6] for Taylor bubble in a stagnant. On figure 6, we present

cross section of the velocity field at the vicinity of the tail which clearly illustrates the turbulent pattern at the wake.

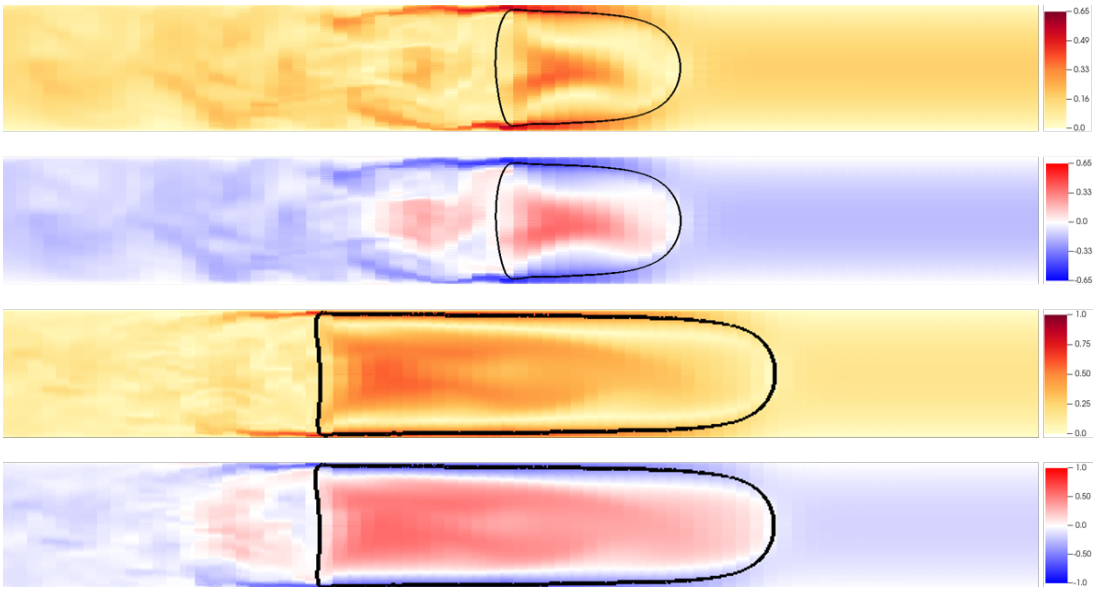

Figure 5: Velocity fields $[m.s^{-1}]$ rotated for visibility, the liquid flowing from the right to the left. From the top to the bottom: velocity magnitude and axial velocity for the 1.5 D long bubble, then for the 3.5 D long bubble.

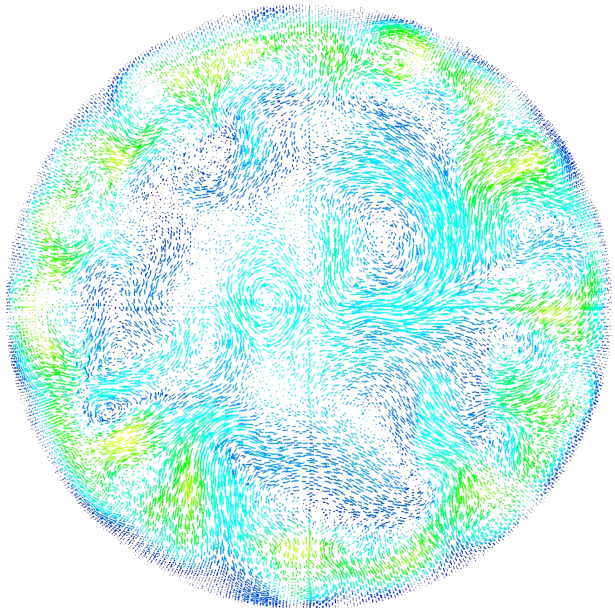

Figure 6: Cross section of the velocity field at 0.5 D from tail of the 1.5 D long bubble.

On figure 7, we present the time-averaged profiles of the axial and radial components of the velocity fields in the wake, 1 D behind the bubble. These profiles are consistent with the literature. On figure 7a, we observe that axial velocity has a plateau at the center and a maximum at $r \simeq 0.3\ D$. We can also observe that at the distance from the bubble, there is small recirculation loop near the wall (positive axial and radial velocity near $r = D/2$).

CONCLUSION

We have realized DNS simulation of Taylor bubbles using the Front-Tracking method. This is a premiere for the investigation of such a configuration: vertical counter-current configuration presenting a turbulent wake, using a water/air mixture. The results were validated using

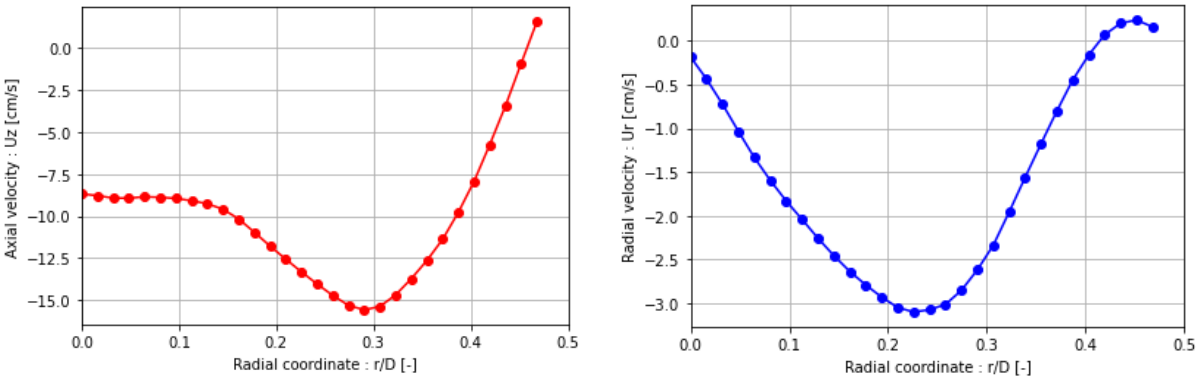

(a) Axial component

(b) Radial component

Figure 7: Average axial and radial velocity profiles at 1 D behind the 1.5 D long bubble

experimental measurements of JSI. Indeed, the bubble rising velocity shows an acceptable discrepancy and the comparison of bubble shapes shows an excellent agreement. We also presented the characteristics of the turbulent bubble wake.

In a future work, further analyses will be realized using PIV measurements produced during this experimental campaign. Particularly, averaged velocity profiles and the statistics of turbulence. This would contribute to a better understanding of the turbulent wake and consolidate the validation of TRUST/TrioCFD. Another aspect to investigate would be the two dimensional oscilation of the tail. Moreover, DNS simulations of Taylor bubbles under turbulent inlet conditions (experimentally presented in [4]) are already on track using the same methodology.

REFERENCES

[1] J. Kren, B. Mikuž, *Analysis of bubble breakup sensitivity on fluid properties using Large Eddy Simulations*, 31th International Conference Nuclear Energy for New Europe (NENE), Portorož, Slovenia, 2022.

[2] J. Kren, I. Tiselj, B. Mikuž, *Bubble Breakup Sensitivity on Local Surface Tension Modification in LES of Turbulent Slug Flow*, 32th International Conference Nuclear Energy for New Europe (NENE), Portorož, Slovenia, 2023.

[3] E.M.A. Frederix, J. Fangb, E. Merzaric, E.M.J. Komen, *High-resolution simulation of turbulent Taylor bubble flow at low Reynolds number*, 11th International Conference on Multiphase Flow (ICMF), Kobe, Japan, 2023.

[4] J. Kren, B. Zajec, I. Tiselj, S. El Shawish, Ž. Perne, M, Tekavčič, B. Mikuž, *Dynamics of Taylor bubble interface in vertical turbulent counter-current flow*, International Journal of Multiphase Flow (IJMF), Volume 165, 2023.

[5] P.-E. Angeli, U. Bieder, G. Fauchet, *Overview of the Trio U code: Main features, V&V procedures and typical applications to engineering*, 16th International Topical Meeting on Nuclear Reactor Thermal Hydraulics (NURETH-16), Chicago, USA, 2015.

[6] J. Campos and J. Carvalho, *An experimental study of the wake of gas slugs rising in liquids*, Journal of Fluid Mechanics, 196, 27-37. 1988.